Determination of Geometrically Necessary Dislocations in Large Shear Strain Localization in Metals

Chaoyi Zhu*, **Veronica Livescu`, Tyler Harrington*, Olivia Dippo*, George T. Gray III`, and Kenneth S. Vecchio***

*Department of NanoEngineering and Materials Science and Engineering Program, UC San Diego, La Jolla CA, 92131

`Los Alamos National Laboratory, Materials Science and Technology Division, Los Alamos, NM 87545

UC San Diego

Los Alamos NATIONAL LABORATORY EST.1943

Shear Localization Tests

Top-hat shape sample

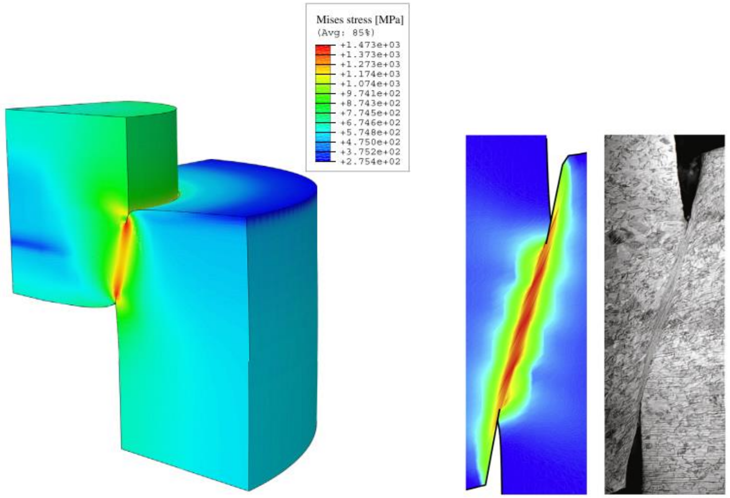

H.M. Mourad *et al*., **2016**

Sample Geometry:

- **Top-hat shape specimen**
- Shear compression specimen
- Double-shear specimen
- Pressure-shear impact test
- etc

Alignment of specific microstructure or texture in hat-shape sample's shear plane is difficult.

Reference:
G.T. Gray III *et al*., Acta Materialia, 2016
Mourad *et al*., International Journal of Plasticity, 2016

Compact forced-simple-shear sample design

Sectioned view of CFSS sample shear zone

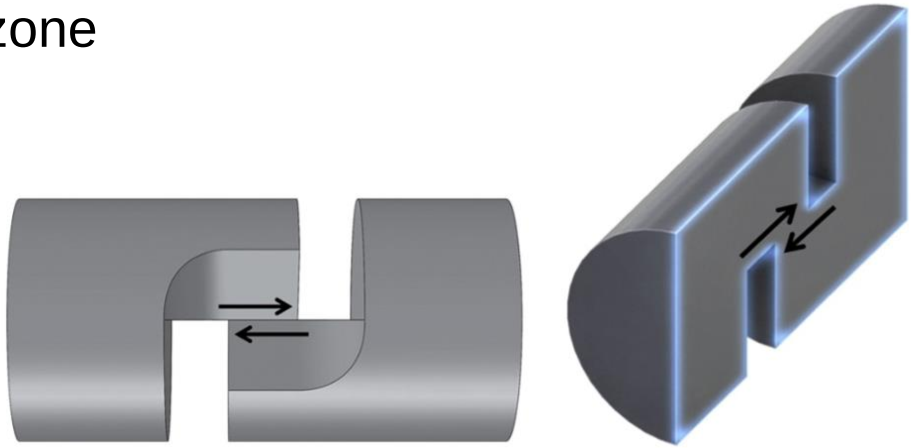

Optical image of shear zone in 7039 aluminium alloy

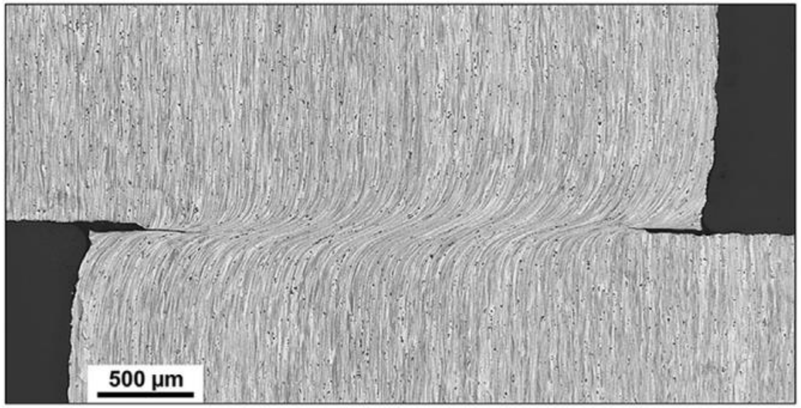

- Alignment of single shear plane during forced shear to specific texture or grain morphology.
- Simple pure shear stress state in the shearing zone
- **Quantify microstructural aspects of shear localization**

Reference: G.T. Gray III *et al*., Acta Materialia, 2016

Overview of EBSD-based GND density calculation

Schematic of Geometrically-necessary (GND) and Statistically-stored (SSD) dislocations

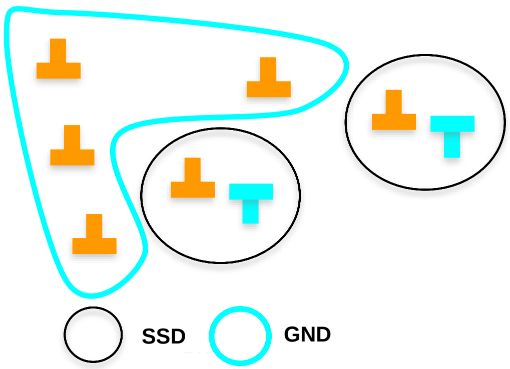

GND in a crystal (e.g. bending)

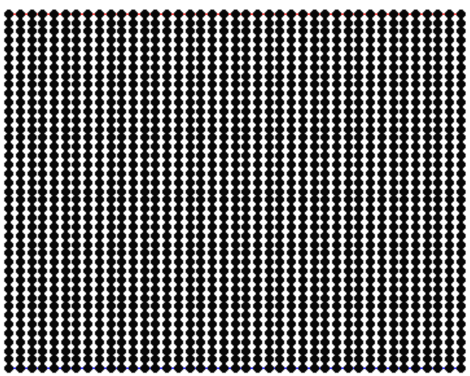

- Accommodate lattice curvature associated with non-uniform deformation
- Obstacles to motions of SSD (hardening)

Nye's dislocation density tensor relates lattice orientation gradients to dislocation density (Nye 1953)

$$\alpha_{ij} = \sum_{n=1}^{N} \rho_{GND}^{n} b_i^n l_j^n$$

$$\alpha = \begin{bmatrix} \frac{\partial\omega_{12}}{\partial x_3} - \frac{\partial\omega_{13}}{\partial x_2} & \frac{\partial\omega_{13}}{\partial x_1} & \frac{\partial\omega_{21}}{\partial x_1} \\ \frac{\partial\omega_{32}}{\partial x_2} & \frac{\partial\omega_{23}}{\partial x_1} - \frac{\partial\omega_{21}}{\partial x_3} & \frac{\partial\omega_{21}}{\partial x_2} \\ \frac{\partial\omega_{32}}{\partial x_3} & \frac{\partial\omega_{13}}{\partial x_3} & \frac{\partial\omega_{31}}{\partial x_2} - \frac{\partial\omega_{32}}{\partial x_1} \end{bmatrix}$$

Extract the lattice orientation gradients (Demir *et al*. 2009)

$$\alpha_{ik} = -\epsilon_{klj}\frac{\partial\beta_{ij}^{el}}{\partial x_l} \approx -\epsilon_{klj} g_{ij,l}$$

Solve for dislocation density vector ρ using Matlab under the the L_1 dislocation energy minimization scheme (Britton *et al.* 2012)

$$\boldsymbol{\alpha} = \boldsymbol{\xi}(6\times33)\cdot\boldsymbol{\rho}(33\times1) = \boldsymbol{\Lambda}(6\times1) \qquad \text{HCP(N=33)}$$

GND resolution is limited by angular resolution and step size (Wilkinson and Randman, 2010)

Reference:
Zhu *et al*., Acta Materialia, 2016
Nye, Acta Metallurgica,1953
Demir *et al*., Acta Materialia, 2009
Britton *et al.*, Acta Materialia, 2012
Wilkinson *et al.*, Philosophical Magazine, 2010

Morphological anisotropy study

Materials specification (7039-Al alloy):

- CFSS samples used by Gray *et al. (2016).*

Loading condition:

- quasi-statically compressed at a strain rate of 0.001/sec at 298K

Slip systems (N=18): <110>{111} 6 screw and 12 edge

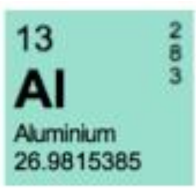

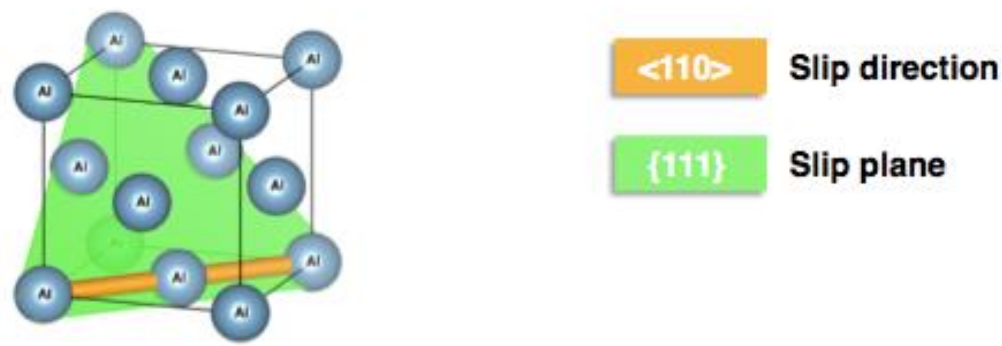

Reference:
G.T. Gray III *et al*., Acta Materialia, 2016
Zhu *et al*., Acta Materialia, 2016

Mechanical response and damage evolution

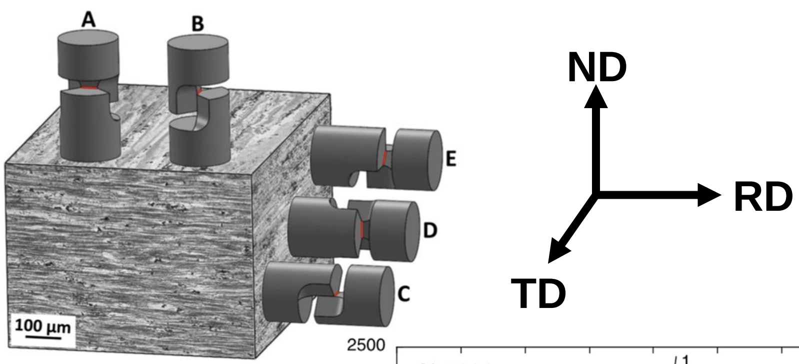

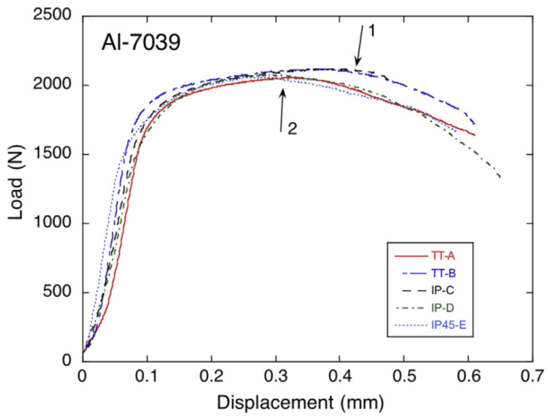

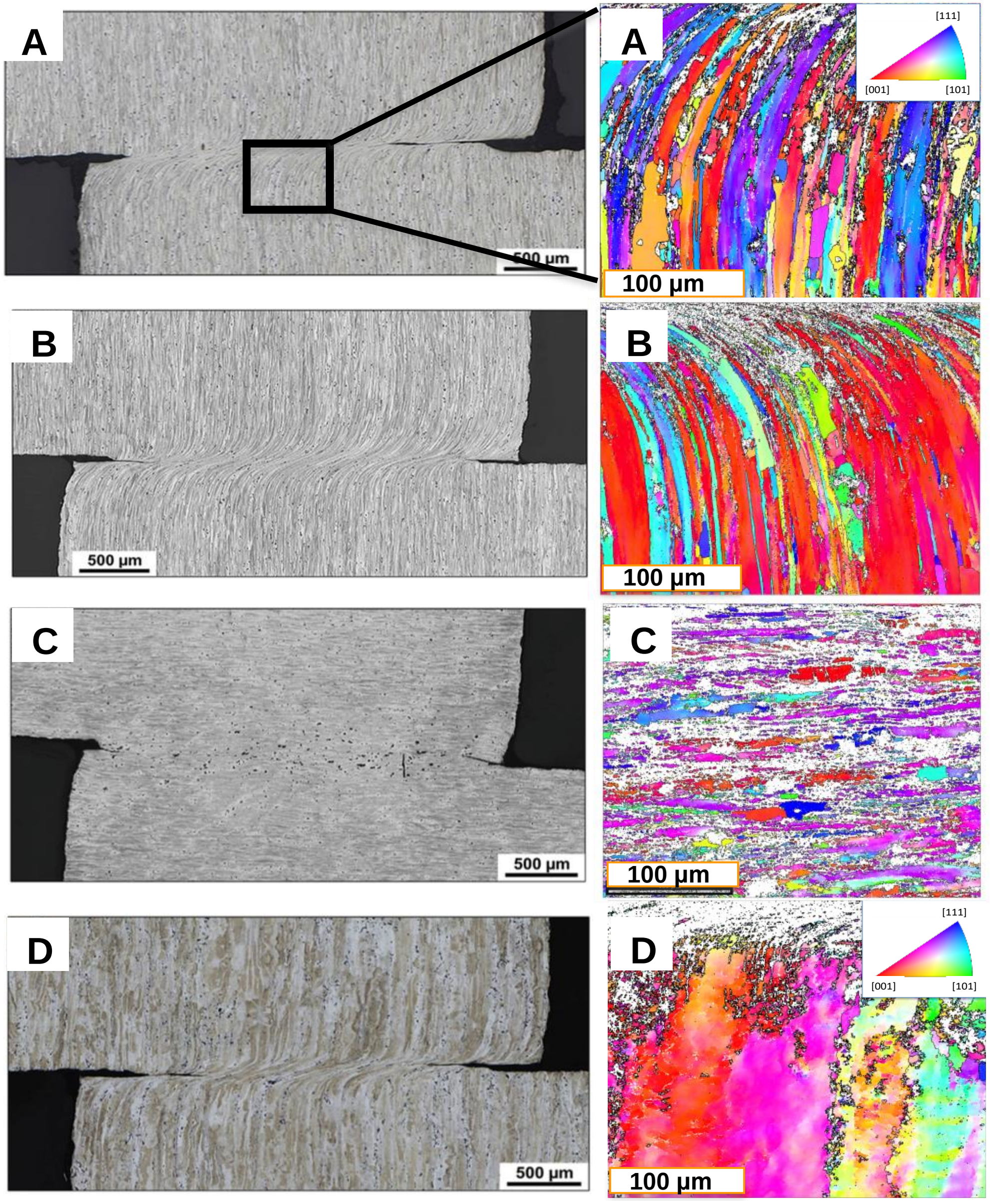

Mechanical response:

- Load displacement response are nominally similar for four samples
- B and C retain higher peak loads at greater level of shear displacement.

Reference:

G.T. Gray III *et al*., Acta Materialia, 2016

Zhu *et al*., Acta Materialia, 2016

Line average GND density method

- Estimate the gradient in GND density over the region of shear localization

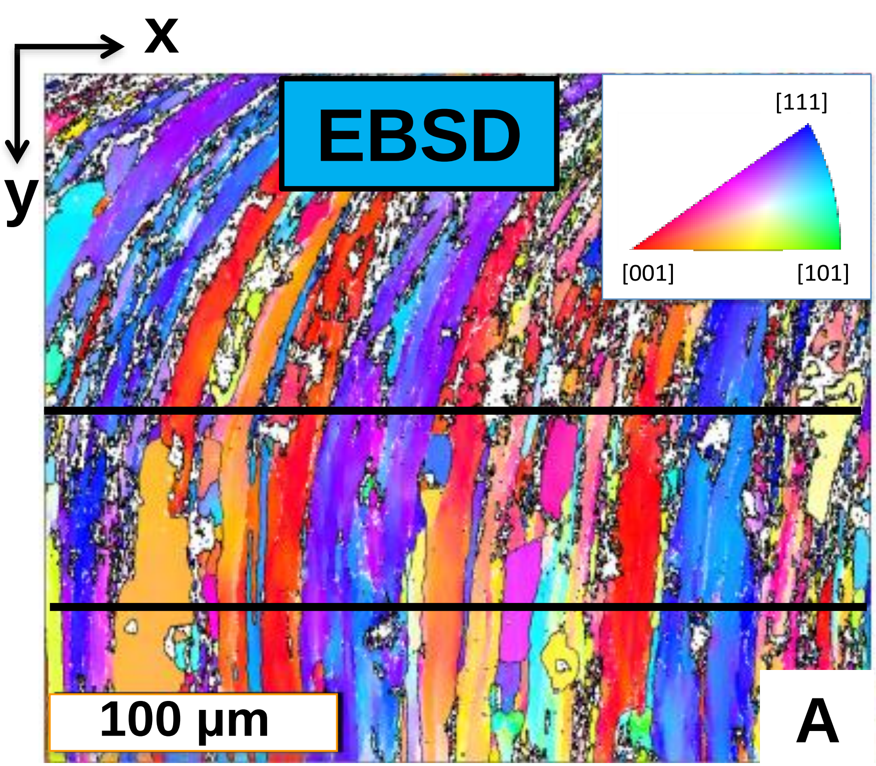

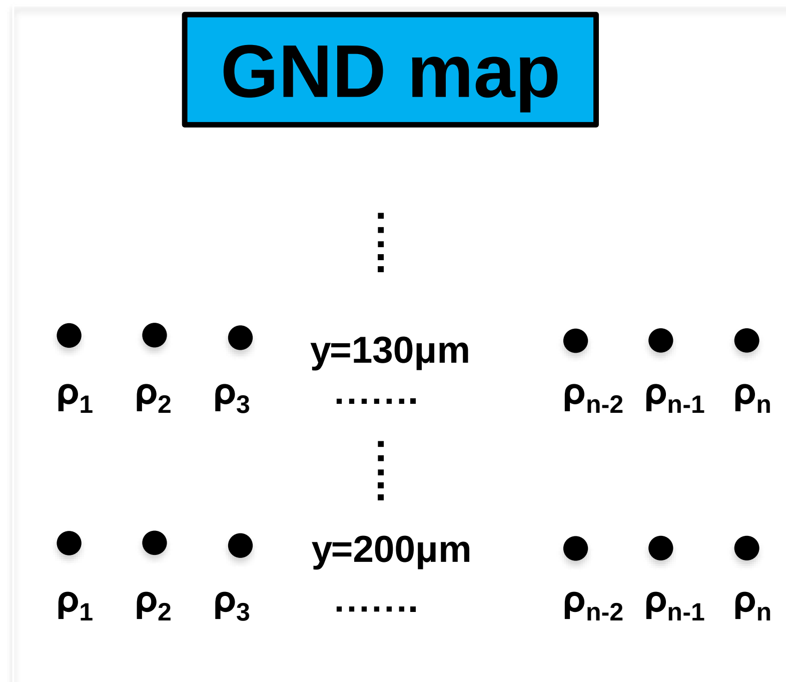

Reference: Zhu *et al.*, Acta Materialia, 2016

‘Shielding effect’ (A-direction)

- Stress-relief crack formation along grain boundary
- Lower grain is ‘shielded’ from shear deformation

Microbands formation (D-direction)

- Multiple microbands formed in the direction of shear
- Local GND density peaks of similar order of magnitude

Zhu *et al*., Acta Materialia, 2016

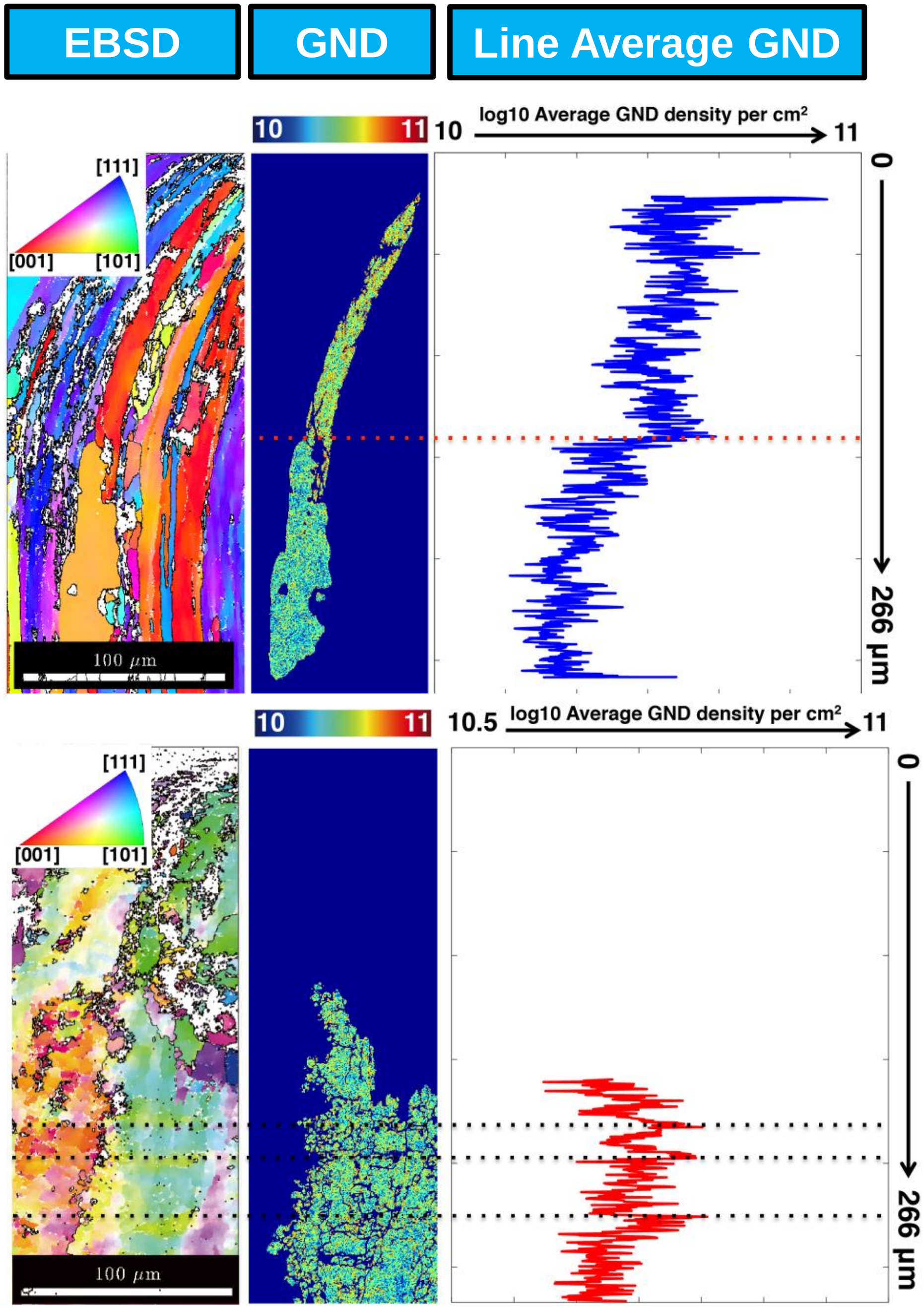

Grain shape effect (B-direction)

- Due to geometric constraint,GND density varies inversely to the slip distance (Ashby, 1970) i.e. horizontal distance across the grain in the direction of shear

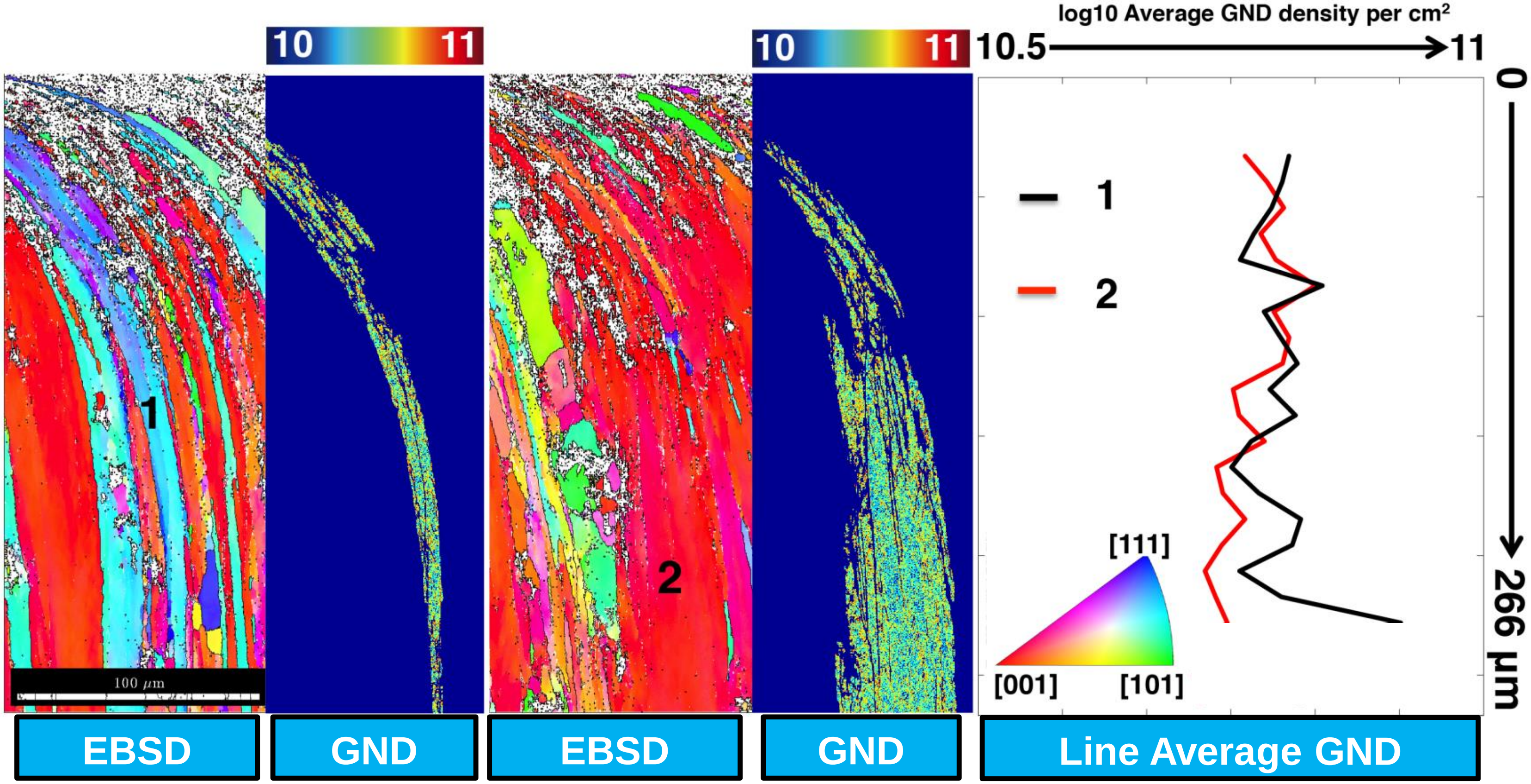

Ashby, Philosophical Magazine, 1970
Zhu *et al*., Acta Materialia, 2016

Line average GND density profiles for 7039 aluminium alloy

- Higher GND density close to center of shear band for B-Dir and across the C-Dir, leading to more pronounced strain hardening effect
- The amount of GND decreases away from the shear band center, except for C-Dir
- The amount of GND present are very similar for A-, B- and D-Dir away from shear band, and more edge-type GND are present than screw-type GND

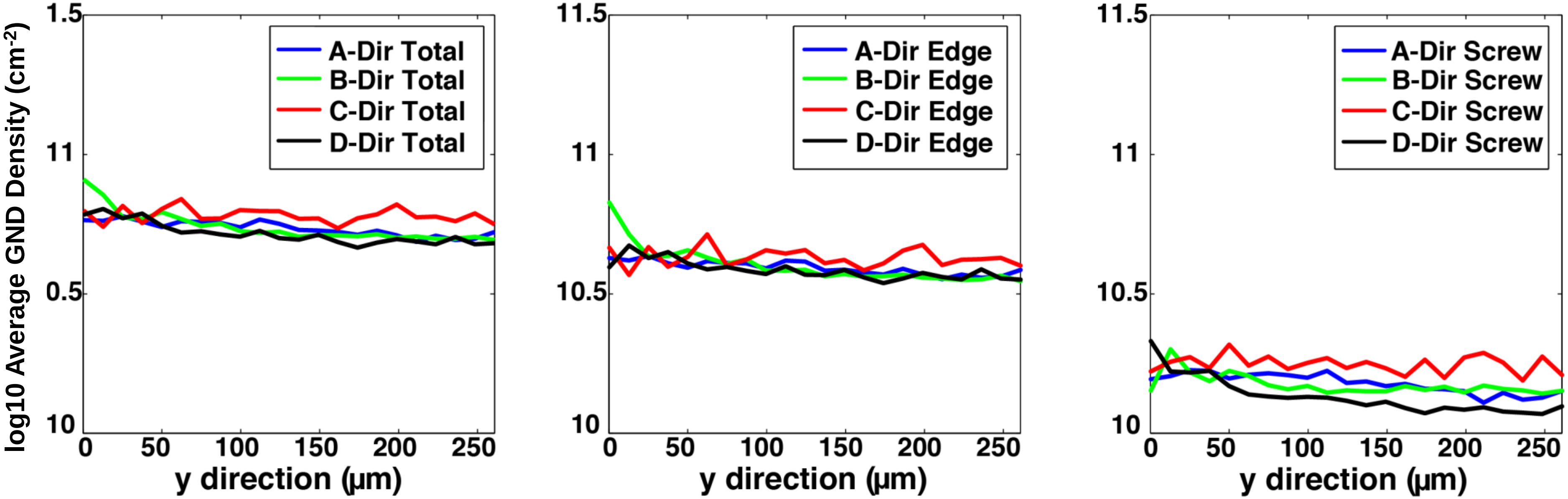

Zhu *et al*., Acta Materialia, 2016

Crystallographic anisotropy study

Materials specification (high-purity titanium):

- CFSS samples used by Gray *et al.*

Loading condition:

- quasi-statically compressed at a strain rate of 0.001/sec at 293K.

Slip systems (N=33) (Jones and Hutchinson, 1981):

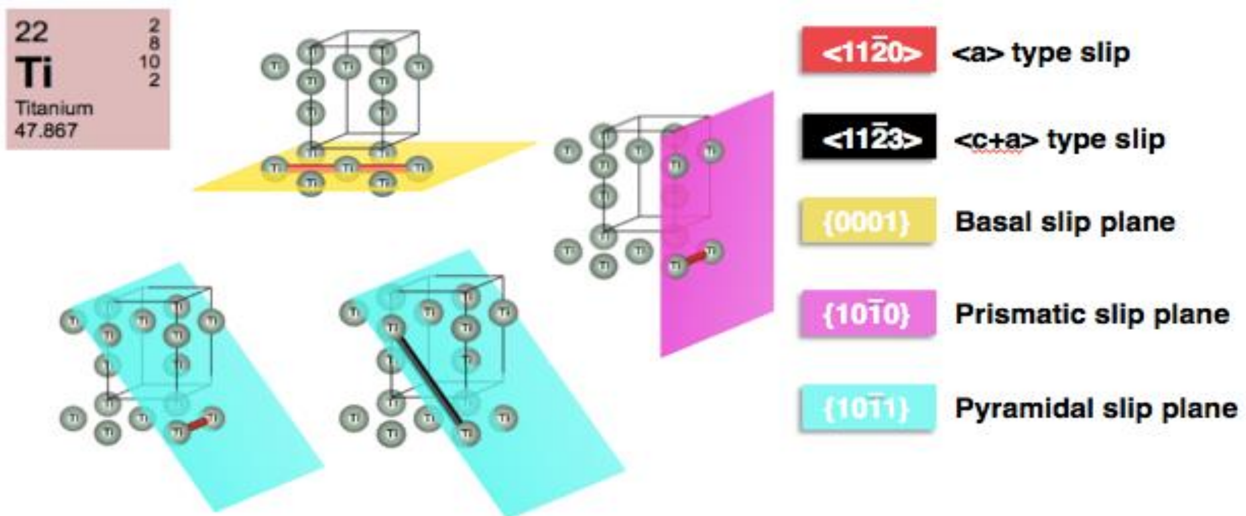

Reference: G.T. Gray III *et al*., Proceedings of the 13th World Conference on Titanium, 2016
Jones and Hutchinson, Acta Metallurgica, 1981

Test sample orientation and texture

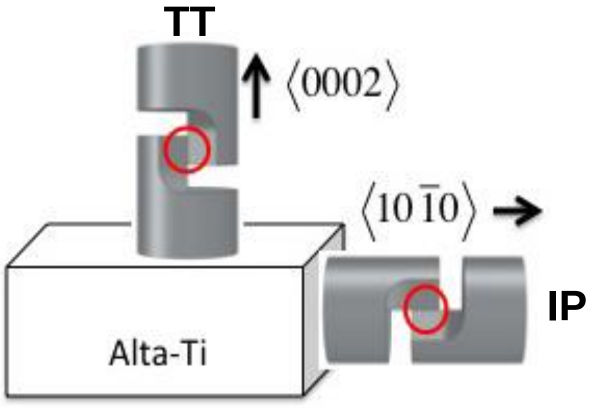

Inverse pole figures of shear planes

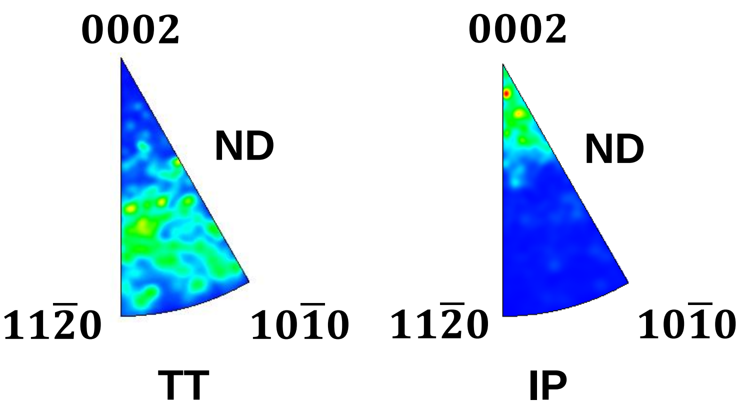

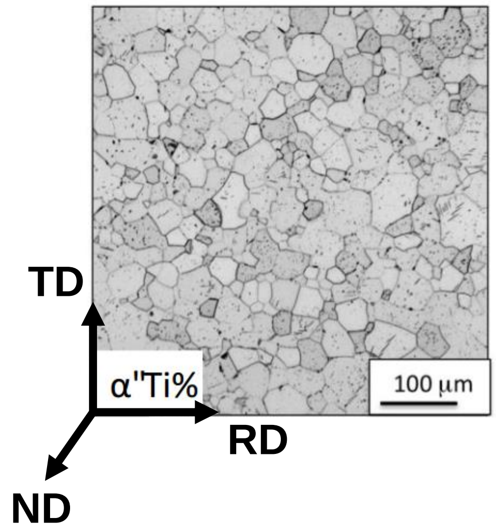

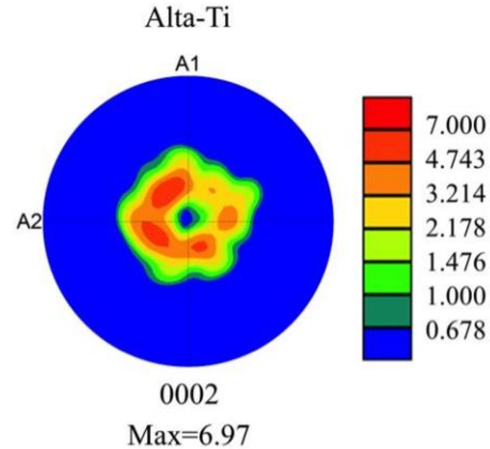

- The [0002] phase-pole figure showing strong texture in the plane of the plate

Reference:
G.T. Gray III *et al*., Proceedings of the 13th World Conference on Titanium, 2016

Mechanical response and shear band formation

- High strain hardening rate for both samples
- Higher tensile strength for TT sample
- Shear strain achieved for IP sample is higher

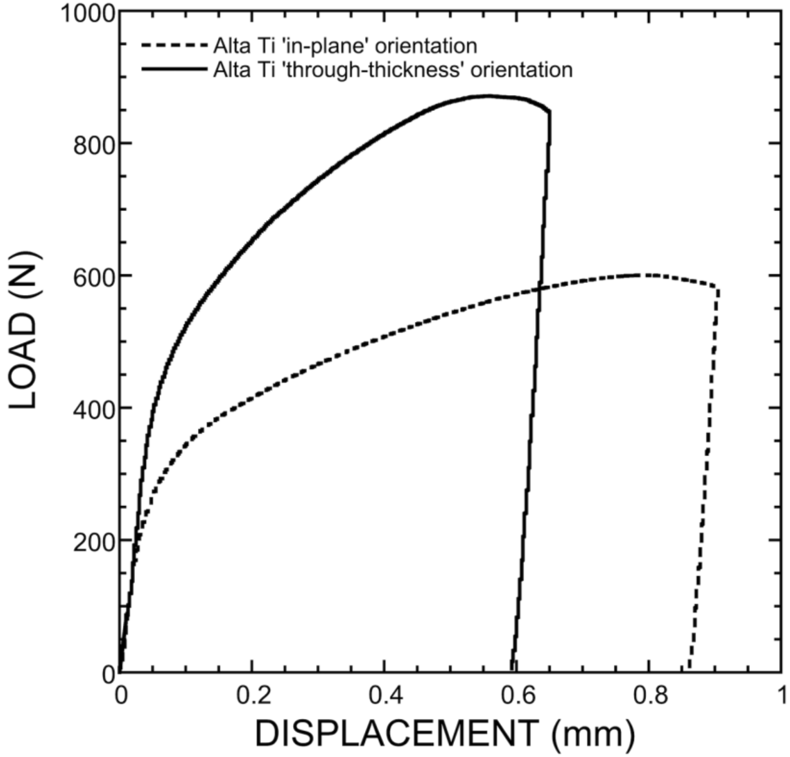

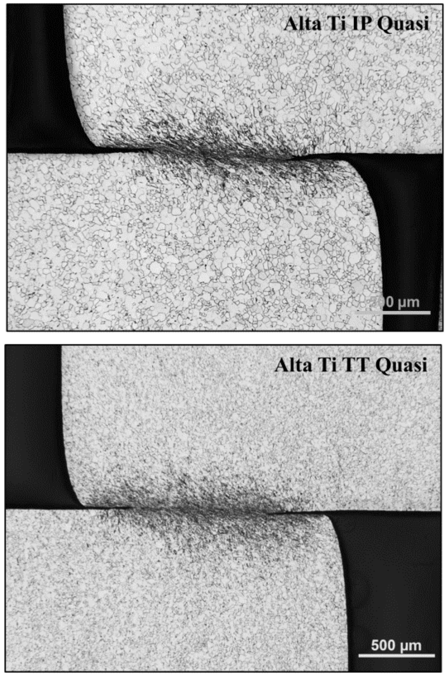

Reference: G.T. Gray III *et al*., Proceedings of the 13th World Conference on Titanium, 2016

Schmid factors under simple shear deformation

$\tau_{RSS} = m \cdot \sigma_{applied}$ Condition for dislocation motion: $\tau_{RSS} \geq \tau_{CRSS}$

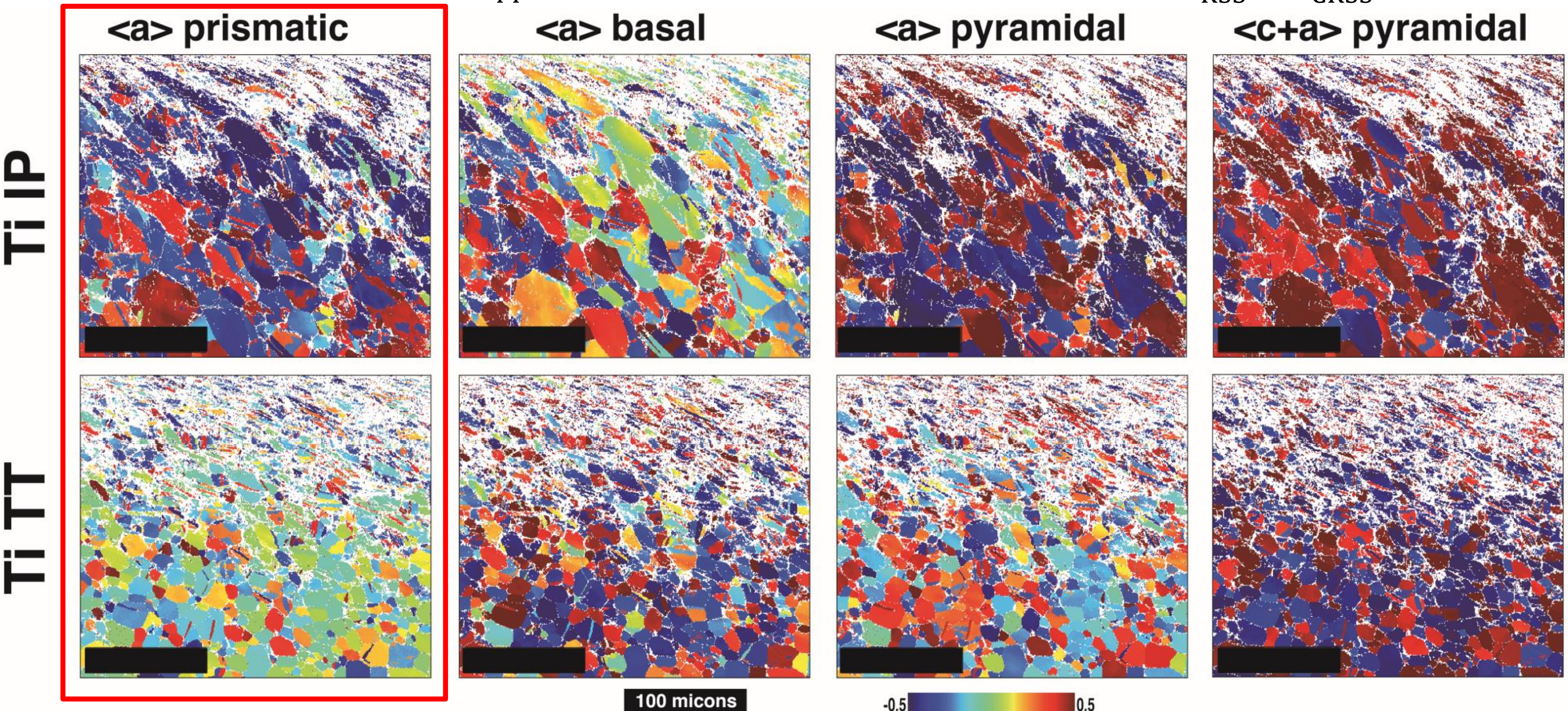

Low CRSS → High CRSS

Reference:
Gong *et al.*, Acta Materialia, 2009
http://mtex-toolbox.github.io/

IP: easy <a> prismatic and pyramidal slips
TT: unfavorable <a> type slips

Distribution of GND density data points for <a> and <c+a> type slips

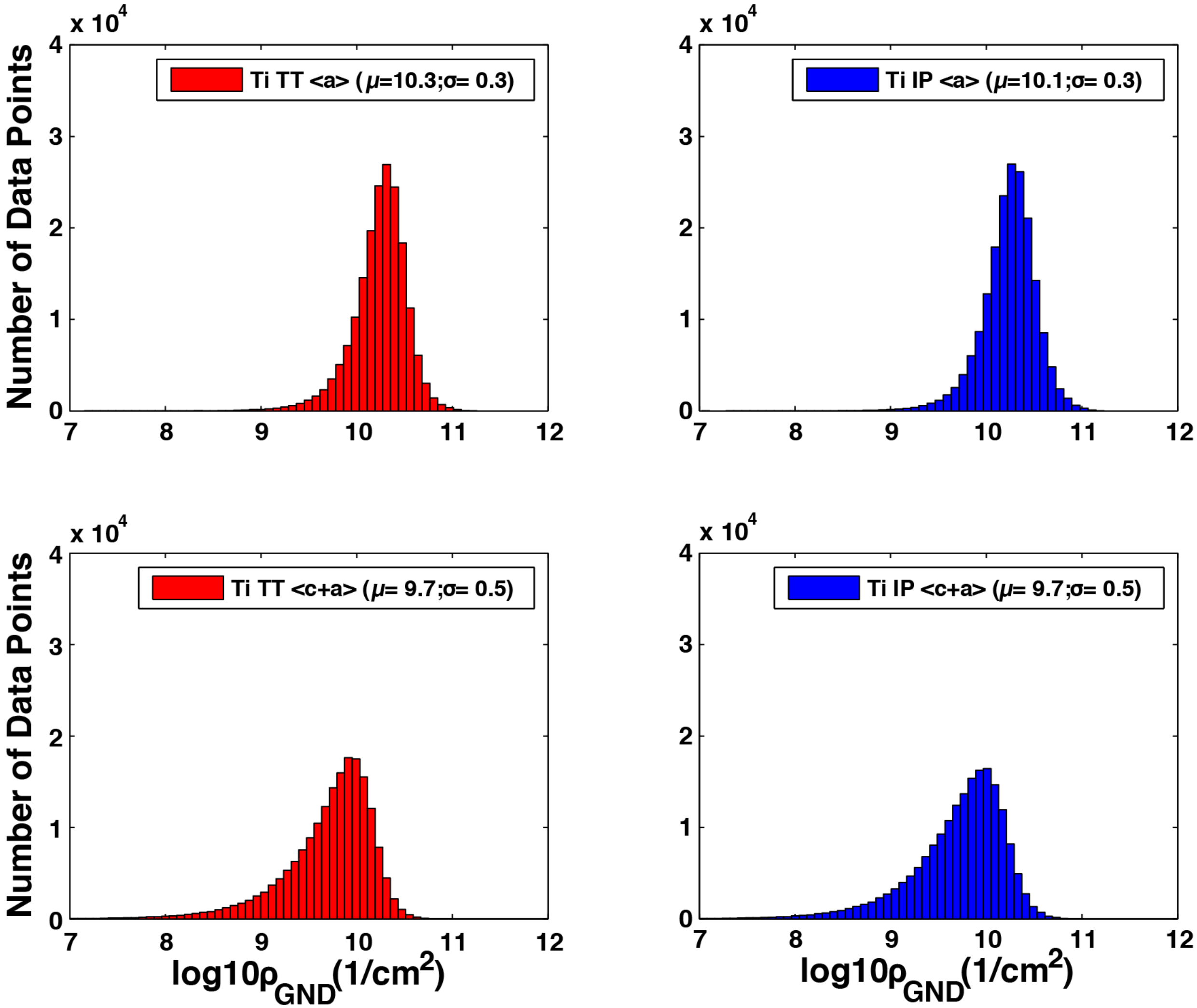

- The number of <a> type GND is much more than the <c+a> type in both samples.
- More statistical variation is present in the <c+a> type slip.
- The <a> type in TT sample is slightly higher than the IP sample.

Orientation dependence of grain average GND in high-purity titanium

- The order of magnitude of grain average GND is linearly dependent on the Φ angle

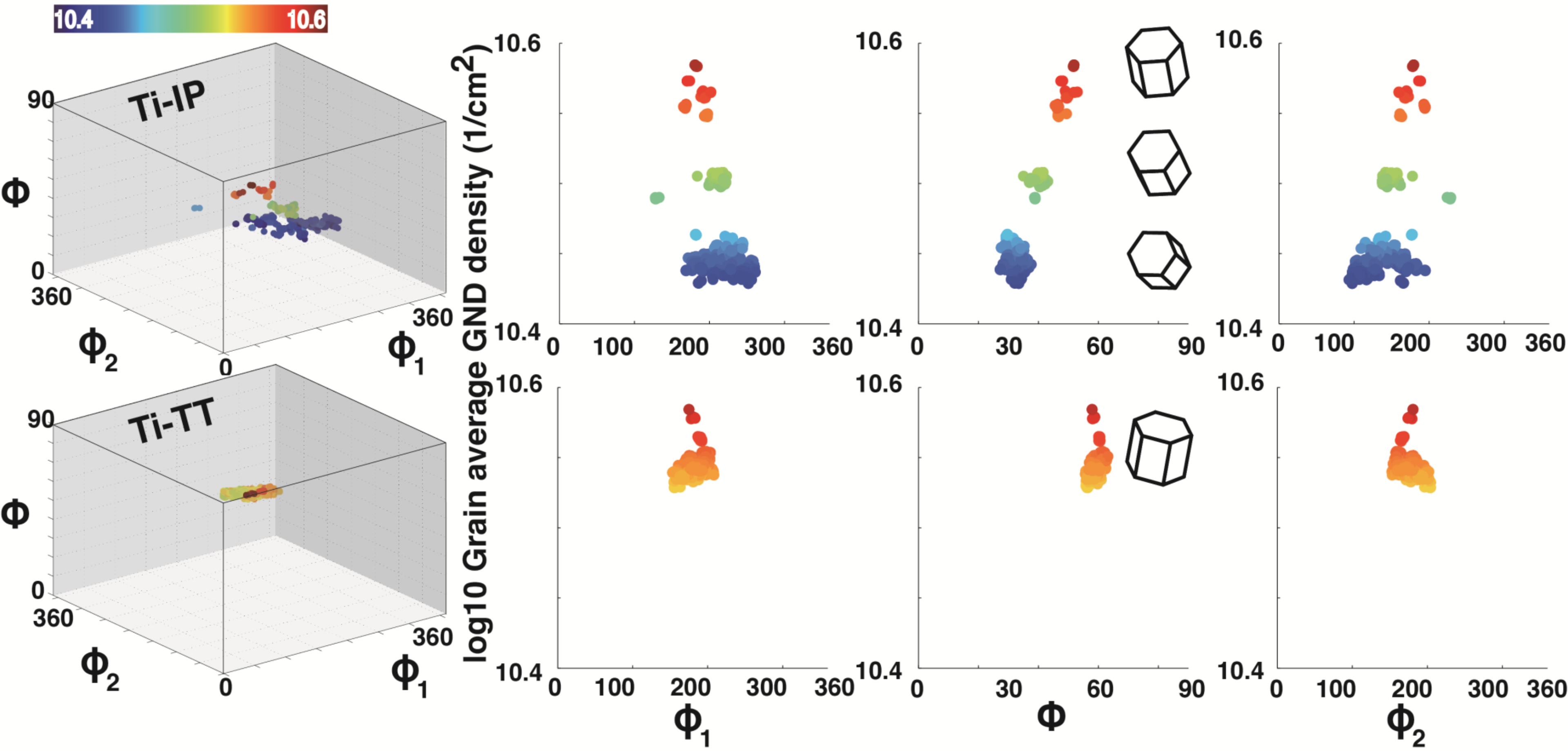

Summary

7039-Al alloy:

i. Anisotropy in damage evolution and shear-stress shear-strain response of 7039-aluminum alloy is associated with the grain structure of the material, i.e. morphological anisotropy creating variations in grain boundary interactions

ii. Microbands formation in D-direction is associated with local GND peaks;

iii. Stress-relief crack propagating along grain boundaries due to the presence of voids or inclusions generates a ‘shielding effect’ on neighboring grains;

iv. Line average GND varies inversely with the width of the grain, leading to generally pronounced higher GND density near triple junctions.

v. Higher GND density close to center of shear band for B-Dir and across the C-Dir, leading to more pronounced strain hardening effect

Summary

High-purity Ti:

i) The anisotropy in deformation response for the high-purity titanium samples are derived from initial crystallographic texture of the materials, in which the IP sample favors easy <a> prismatic and pyramidal slips and TT sample has unfavorable <a> type slip

ii) Total GND and <a> type GND density are higher in TT sample, whereas the <c+a> type GND are similar in magnitude for both.

iii) More <a> type GND remained in both samples than <c+a> type GND.

iv) the increase in grain average GND density was determined to have strong correlation to increase in the Φ angle of the grain average orientation

Thank you!

Orientation dependence of grain average GND in aluminum

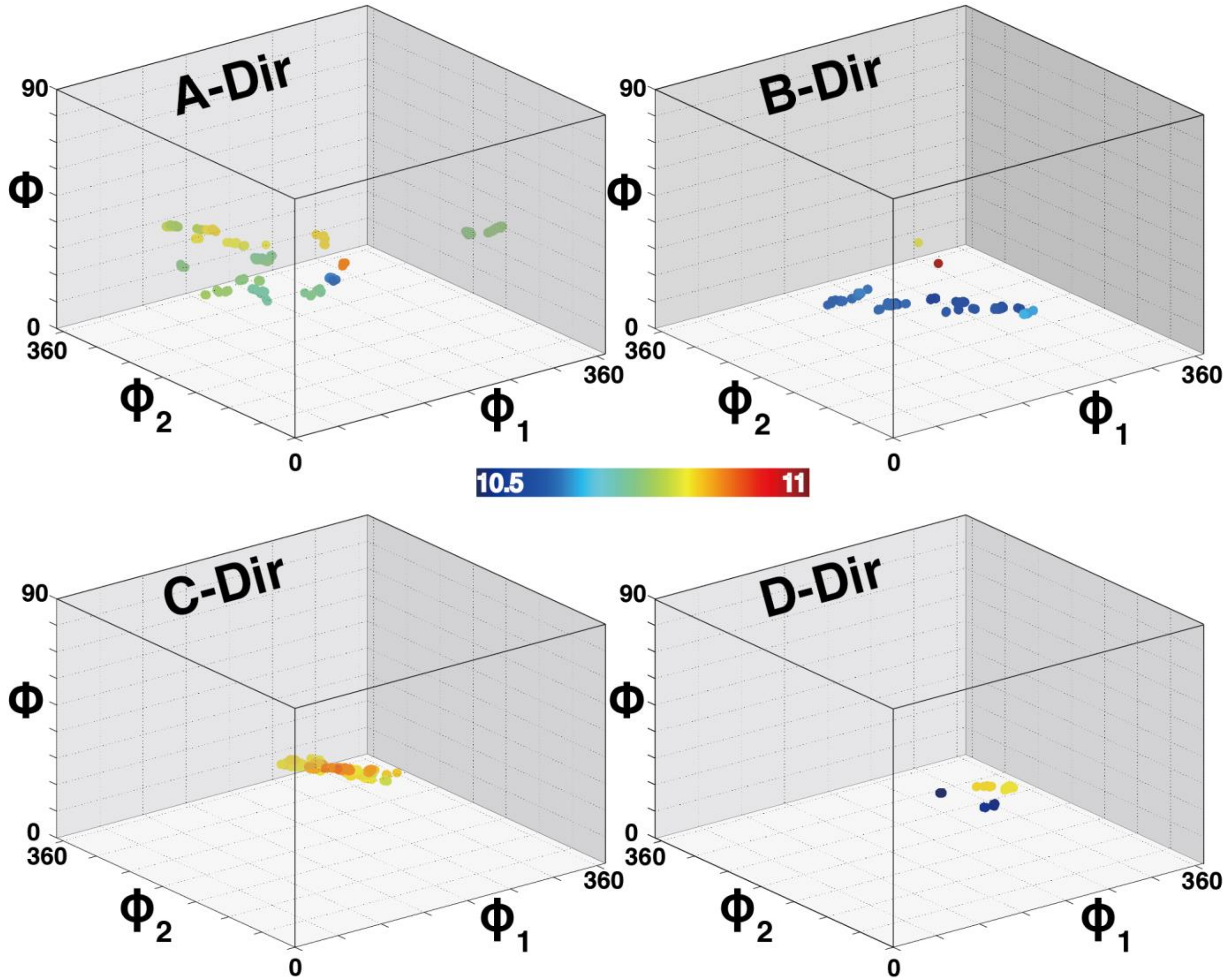

Pattern degradation effect on the number of available GND data points

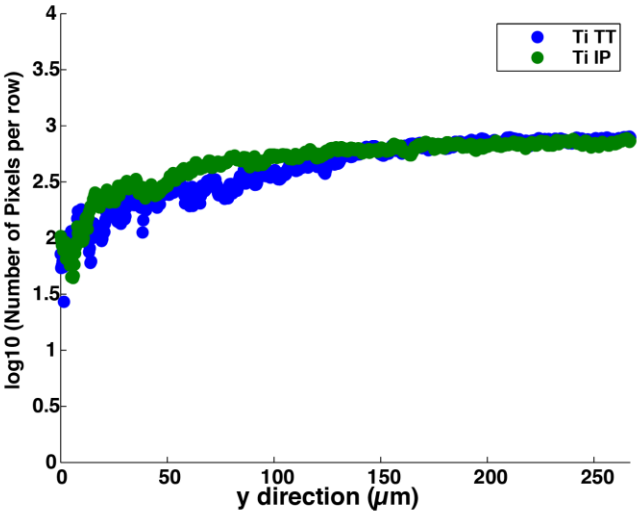

- Amount of GND present is higher in TT
- The width of shear band is wider in TT

EBSD images and selected GND maps

- Noise floor 5×10^9 per cm^2

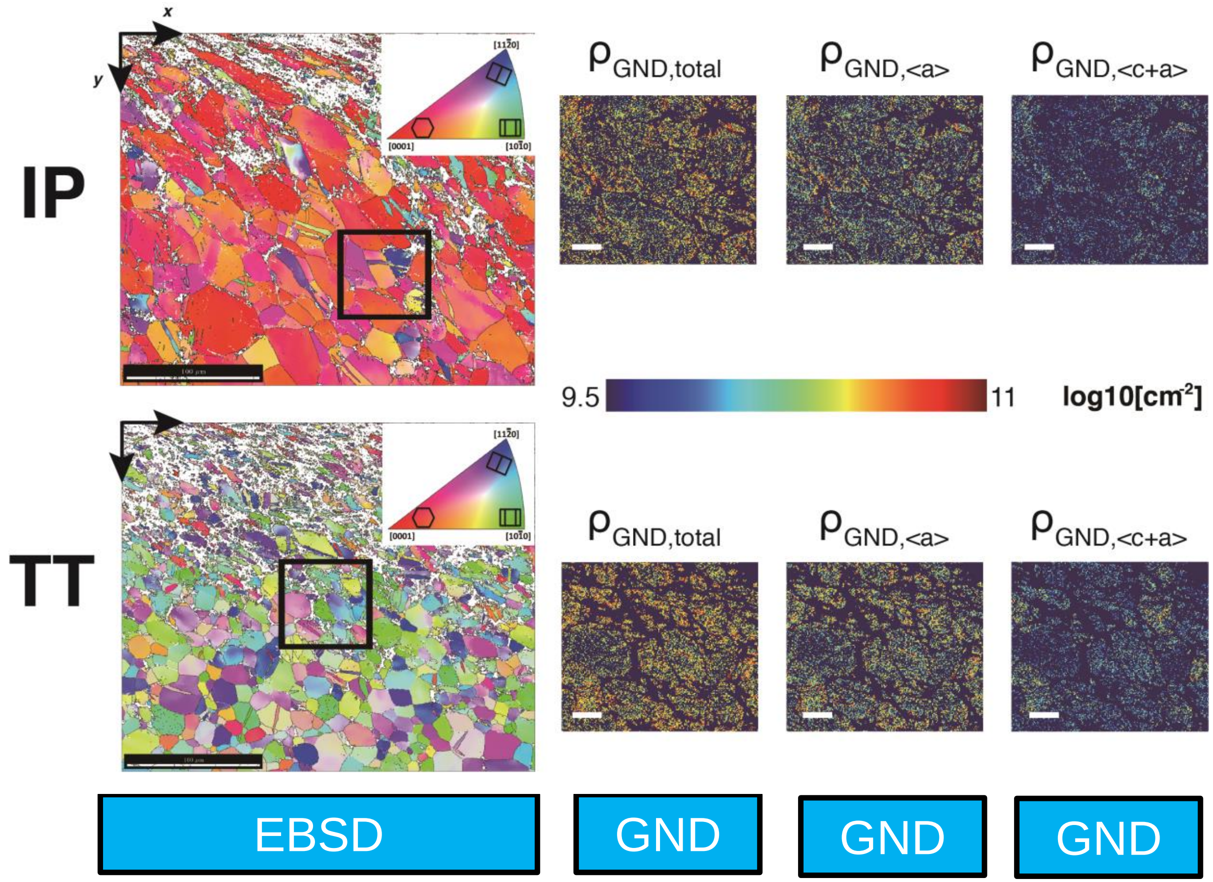

Backup slides

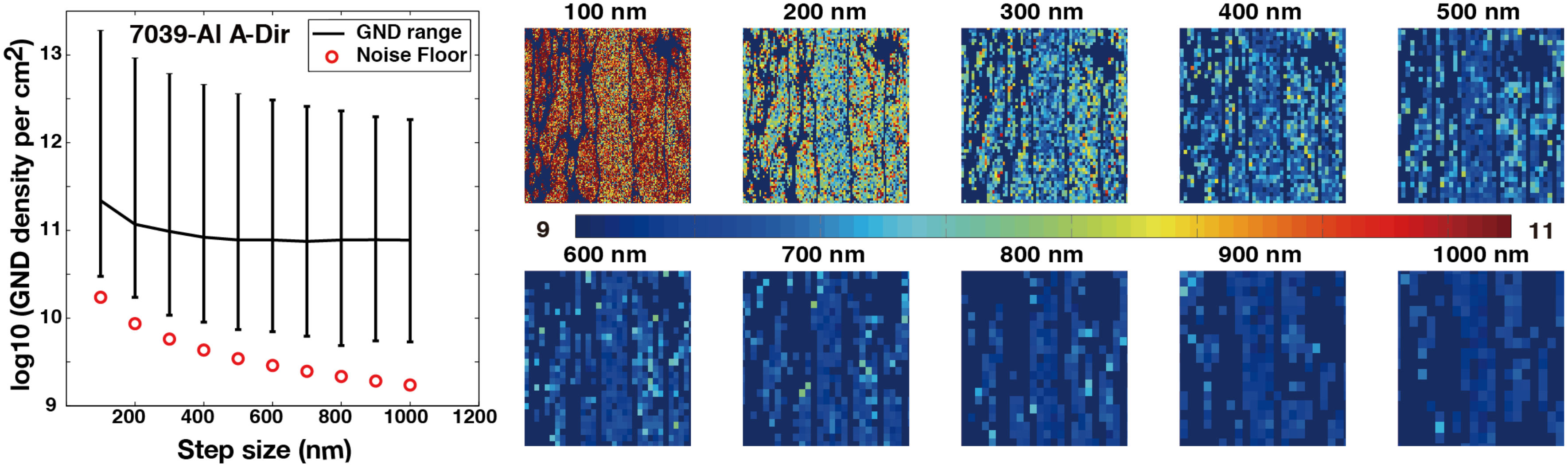

Left: Step size analysis for 7039-aluminum samples, machined from the A-direction. Black curve is the mean GND density of the selected area as a function of step size (nm); Black error bars represent the range of GND density values spanned at each step size; red circles denote the noise floor estimated at every step size with a corresponding angular resolution of 0.4° and Burgers vector of 2.86 Å for aluminum; Right: GND maps in step size dependence analysis for the same selected area of 7039-aluminum A-direction sample (size of the box is 25 mm by 25 mm) at step sizes of 100 nm, 200 nm, 300 nm, 400 nm, 500 nm, 600 nm, 700 nm, 800 nm, 900 nm, and 1000 nm (log10 scale, unit: 1/cm2). (For interpretation of the references to color in this figure legend, the reader is referred to the web version of this article.)

Line average GND density profiles for shear bands in high-purity titanium

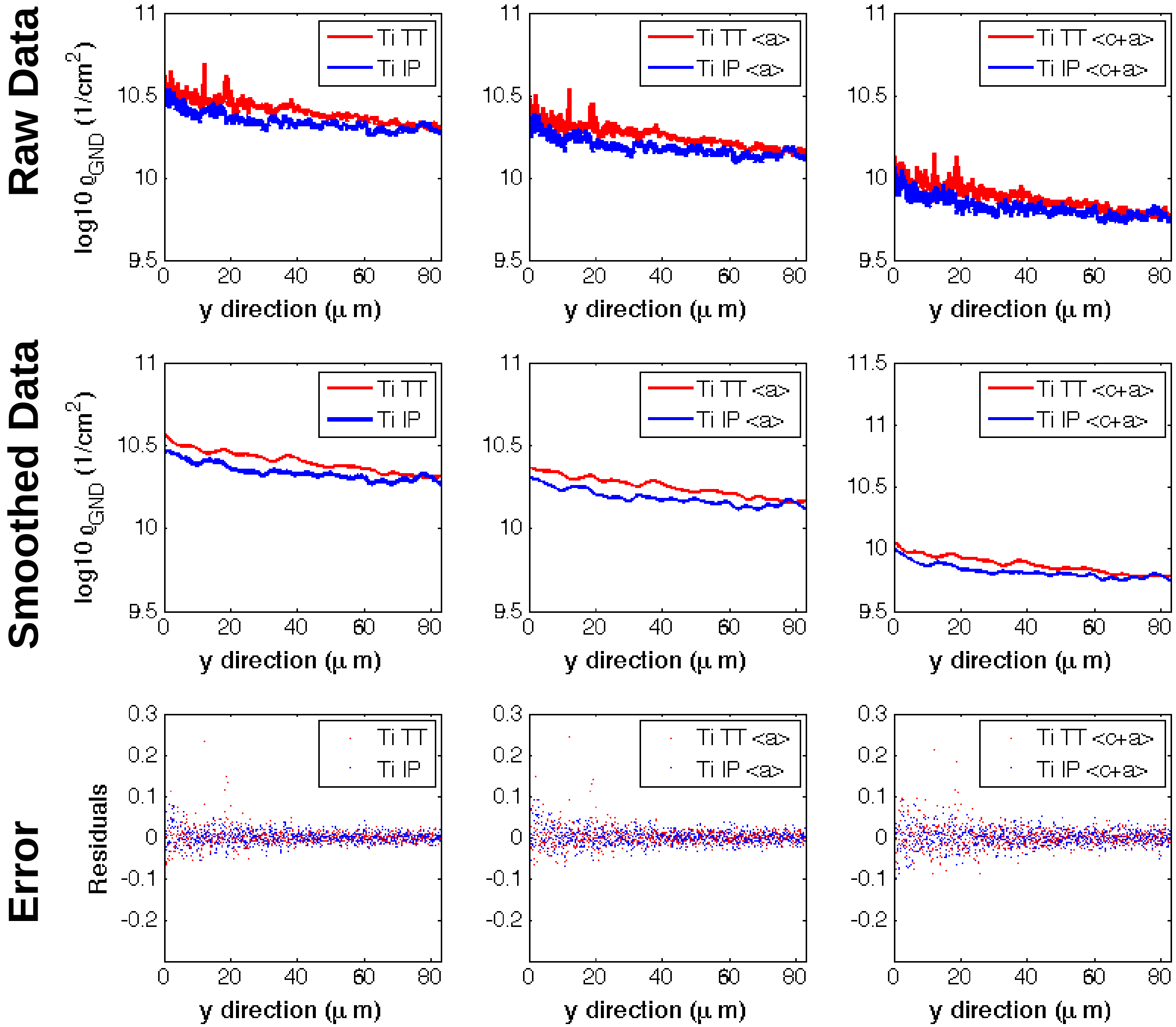

- Higher total and mainly <a> type GND density for TT sample close to the center of shear band due to shearing of less favorably oriented grains.
- More <a> type GND remained in both samples than <c+a> type GND.
- <a> type GND drops at a faster rate than <c+a> type GNDs, strain-hardening of high-purity titanium is mainly through <a> type.

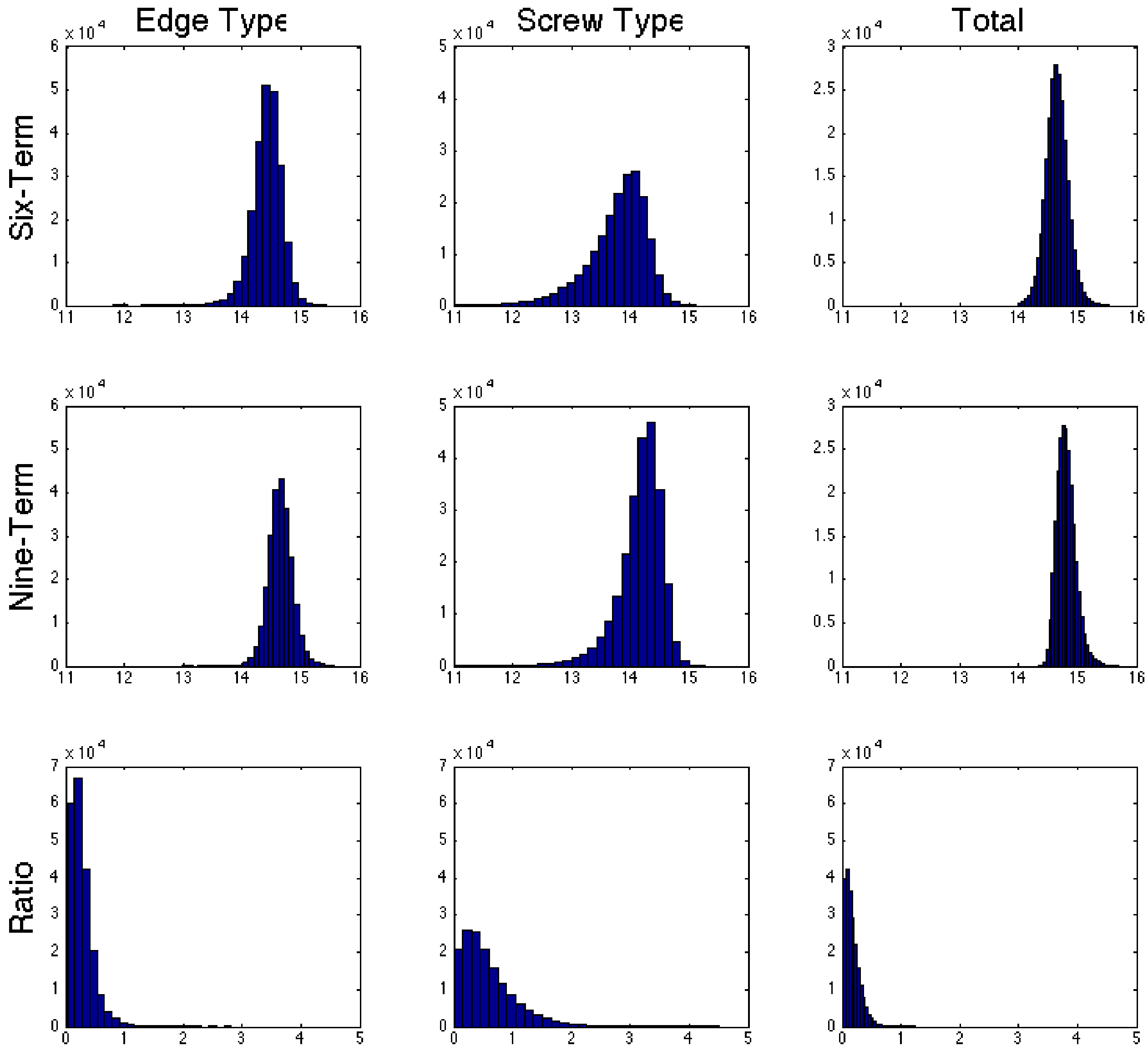

Comparison of effect to six term and nine term approaches on GND density distributions in FCC crystal.

Orientation dependence for <a> and <c+a> type in TT sample

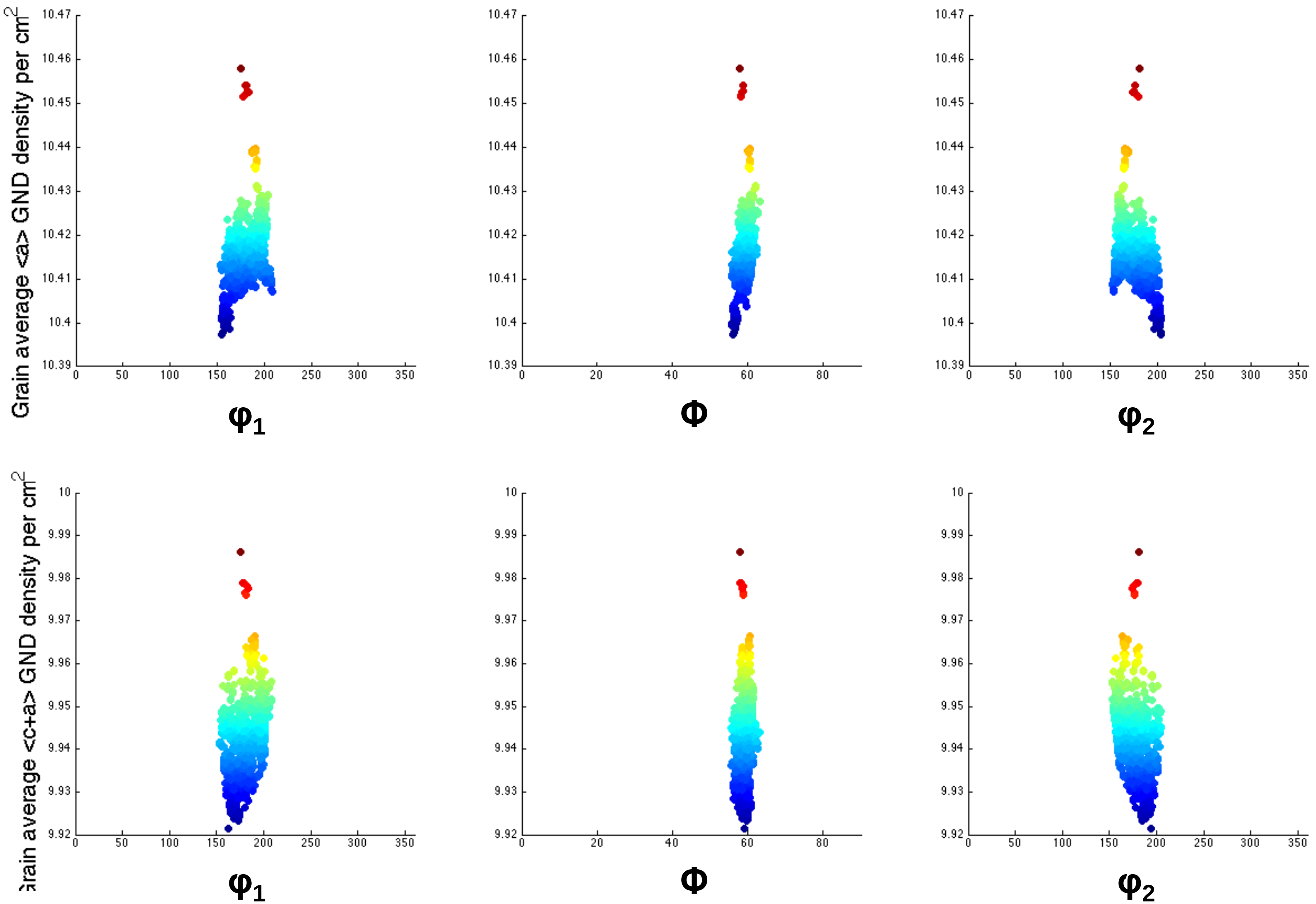

Orientation dependence for <a> and <c+a> type in IP sample

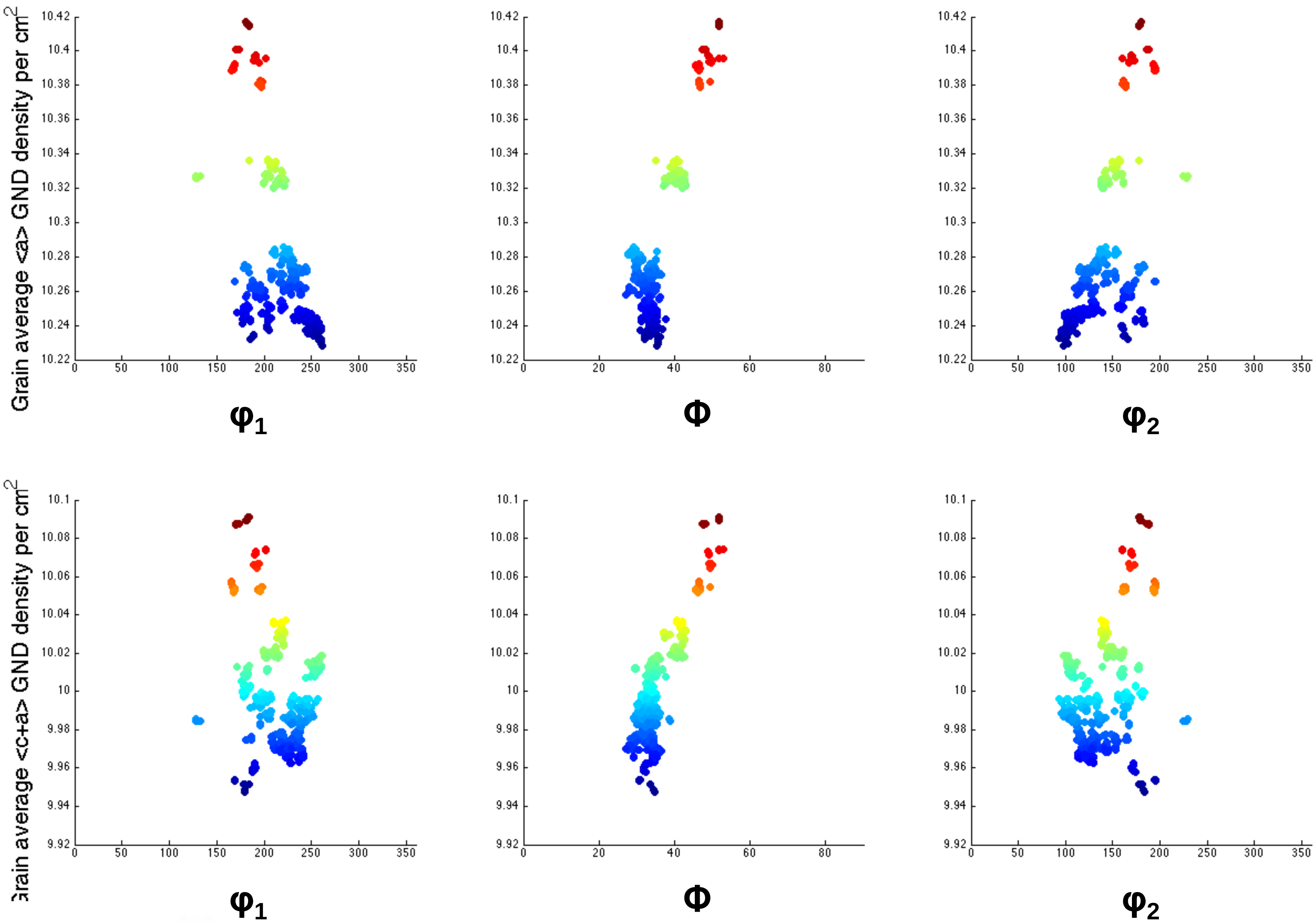

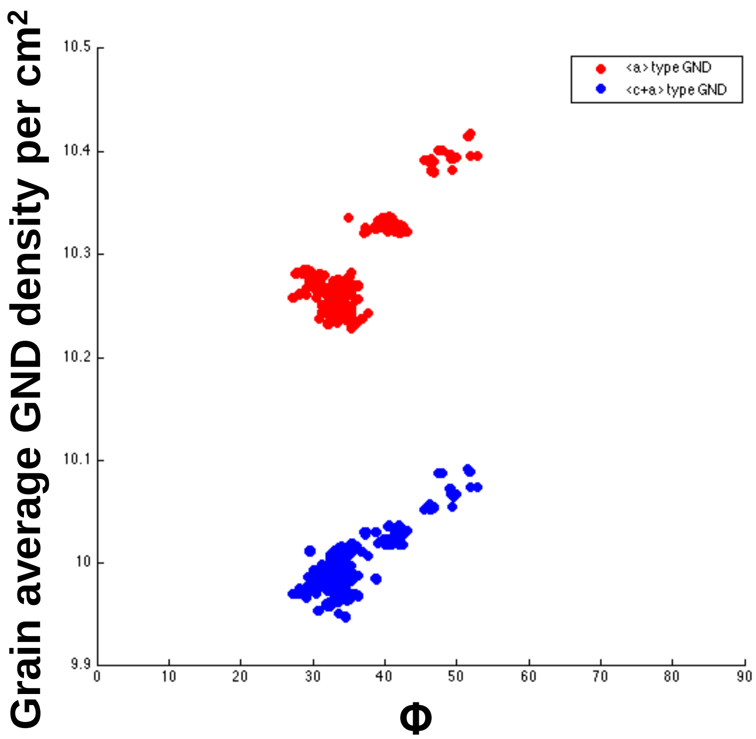
Grain average GND density per cm²
10.5
10.4
10.3
10.2
10.1
10
9.9
0
10
20
30
40
50
60
70
80
90
<a> type GND
<c+a> type GND
Φ

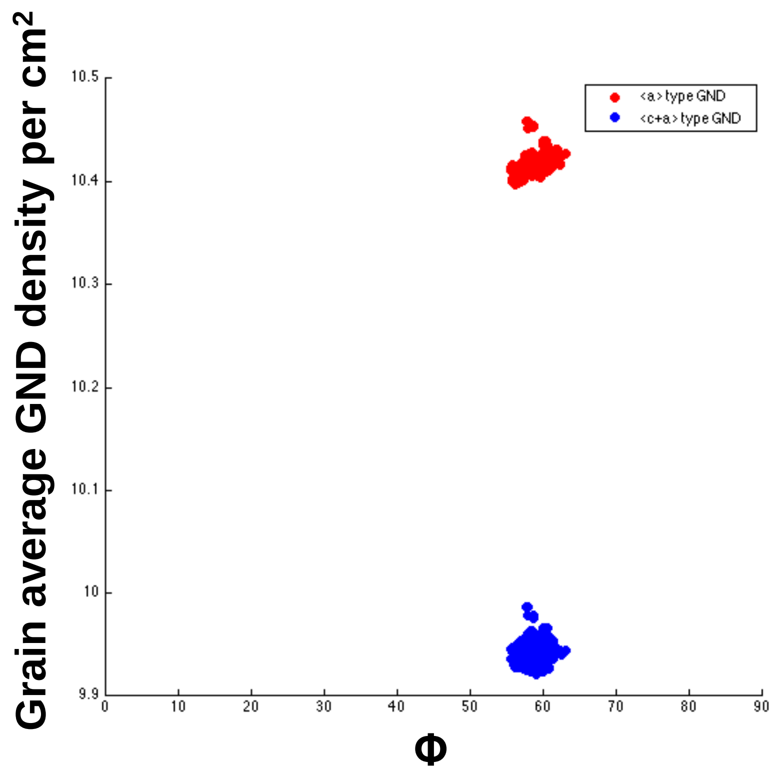
Grain average GND density per cm²
10.5
10.4
10.3
10.2
10.1
10
9.9
0
10
20
30
40
50
60
70
80
90
<a> type GND
<c+a> type GND
Φ